Advances in Materials Research, *Vol. 14, No. 6 (2025) 557-573*
https://doi.org/10.12989/amr.2025.14.6.557

Mechanical and nonlinear hyperelastic behavior of EPDM/ Glass Fiber/Graphene Nanoplatelets hybrid composites: Experimental characterization and analytical modeling

Marwah Sabah Fakhri[1], Sarah Abdul Kadhim[2], Emad Kadum Njim*[3,4] and Royal Madan[5]

[1]*Ministry of Higher Education and Scientific Research-Baghdad, Iraq*
[2]*Materials Engineering Department, Faculty of Engineering, University of Kufa, Iraq*
[3]*Ministry of Industry and Minerals, State Company for Rubber and Tires Industries, Iraq*
[4]*Department of Mechanical Power Engineering, College of Technical Engineering, University of Al Maarif, Al Anbar,31001, Iraq*
[5]*Department of Mechanical Engineering, Graphic Era (Deemed to be University), Dehradun 248002, Uttarakhand*

(*Received September 14, 2023, Revised December 19, 2025, Accepted December 22, 2025*)

Abstract. The study investigates a hybrid composite of Ethylene Propylene Diene Monomer (EPDM) rubber, short glass fibres, and graphene nanoplatelets (GNPs) to improve tensile strength, wear resistance, and nonlinear elastic behaviour. Specimens were prepared by compression molding and tested for tensile and wear performance. Stress–strain behaviour was analyzed using Neo-Hookean, Mooney–Rivlin, and Ogden models, with parameters determined through MATLAB optimization. The work combines EPDM rubber, short glass fibres, and GNPs for enhanced mechanical properties and applies comparative modelling using established constitutive models. The statistical analysis is conducted using one-way ANOVA to validate both experimental and analytical solutions. The hybrid composite showed a 110% increase in tensile strength and a 45% reduction in wear loss compared to pure EPDM. The Mooney–Rivlin model gave the lowest fitting error among the models considered. The MATLAB script developed can be used to predict stress–strain behaviour and assist in the design of similar composites for industrial use.
Keywords: hyperelastic models; mechanical tests; nanofiller; rubber composites; stress-strain behavior

1. Introduction

Rubber-based composites have garnered considerable attention due to their flexibility, damping properties, and wide range of industrial applications. However, pure rubber suffers from low tensile strength and wear resistance, which can be improved by hybrid reinforcement using fibres and nanofillers. Rubber composites are widely used in the automotive, aerospace, and biomedical industries due to their excellent elasticity, vibration damping, and energy absorption. However, their low mechanical strength and wear resistance limit their applications. Fiber reinforcement, such as the addition of glass or aramid fibres, significantly enhances the tensile and fatigue properties of rubber materials (Goodwin and Woods 2025, Njim *et al*. 2024). Recently, the incorporation of nanofillers, such as graphene nanoplatelets (GNPs), silica nanoparticles, or carbon nanotubes

*Corresponding author, Professor, E-mail: emad.kadum@uoa.edu.iq; emad.njim@gmail.com

http://www.techno-press.org/?journal=amr&subpage=5 ISSN: 2234-0912 (Print), 2234-179X (Online)

(CNTs), has led to significant improvements in stiffness, thermal stability, and abrasion resistance (Wang and Lin 2021, Wayzode *et al*. 2025). Hybrid composites that integrate rubber, thermoplastic, and nanofillers represent a novel material class that combines the benefits of macro and nano-reinforcement. Such systems have potential applications in high-performance tires, flexible seals, biomedical prosthetics, vibration isolators, and wearable electronics (Metteb *et al*. 2025, Njim *et al*. 2024). Despite their promising properties, there is a lack of detailed studies on the nonlinear hyperelastic behaviour of such hybrid composites, which is crucial for accurate finite element modelling (FEM) and design. Hybrid composites integrating rubber, fibers, and nanofillers offer a synergistic combination of macro and nano-scale reinforcement. The existing literature focuses mainly on binary systems, detailed investigations of ternary hybrid systems using hyperelastic modeling are scarce. The use of hyperelastic materials, such as natural rubber, synthetic elastomers, and biological materials, is widespread across industries, including petroleum machinery, aerospace, packaging, soft robotics, wearable devices, and biomedical engineering, in both the natural world and everyday life. Material properties, such as their nonlinearities, cause such materials to exhibit large strains under external loads, resulting in deformations and motions that are inherently nonlinear (Xie *et al*. 2024). Researchers have focused on the nonlinear dynamics of both composite and FGM shell structures involving nanocomposite, viscoelastic, and hyperelastic material systems Palani and Swain (2025). An investigation utilizing additive manufacturing to construct solid silicone elastomer sheets with a stretch ratio of up to 2, enabling the measurement and characterization of their mechanical properties under biaxial equi-stretch conditions (Putra *et al*. 2020). An experimental investigation was conducted on the surface modification of abaca fibre using potassium permanganate and sodium hydroxide solutions to enhance crystallinity and reduce its hydrophilicity (Sinha *et al*. 2020). The composite materials industry has recently embraced nanocomposites as an innovative approach to drug, sports, food, and aerospace applications. Recent studies encompass a wide range of subjects (Mohamed *et al*. 2025). A simple hydrothermal process was employed to create a layered hybrid nanocomposite that improves performance across multiple therapeutic applications (Alahmadi *et al*. 2025). Additionally, the review examined the various dimensionalities of Graphdiyne, focusing on its molecular structure, electronic properties, synthesis techniques, and applications (Hamid Ali *et al*. 2025). Furthermore, the literature provides a comprehensive discussion of functionalized nanomaterials for energy applications, with particular emphasis on hydrogen production (Mohamed Salaheldeen *et al*. 2025).

A FEA was conducted to evaluate the fit to the biaxial tensile test results using four hyperelastic material models. An asymptotic numerical method is employed to develop a 3D micromechanical model that describes the behaviour of macromolecular chains and hyperelastic properties of rubber-like materials (Ouardi *et al*. 2025). Polymer nanocomposites are increasingly important in engineering applications involving large deformations. However, the nonlinear behavior of these materials has not been thoroughly studied. (Pelliciari *et al*. 2025) studied a hyperelastic model for nonlinear elastic deformations of graphene-based polymer nanocomposites. Experimental analysis using uniaxial and biaxial tests to show the nonlinear effect of nanoparticles in a silicone matrix on a hyperelastic model.

In (Wang *et al*. 2025), provide detailed information on the complex lubrication of water-lubricated rubber bearings in a comprehensive analysis. This study presents a mixed visco-hyperelastic hydrodynamic lubrication model incorporating viscoelastic dissipation, large nonlinear deformation in rubber friction, and hyperelastic dissipation. Further, (Rodriguez-Piedrahita *et al*. 2025) conducted various tests, including uniaxial compression and tension, simple shear, creep, and relaxation, to investigate recycled rubber simulations as an alternative approach for seismic isolator

testing and performance prediction, aiming to reduce the need for extensive experimental testing through numerical modeling. The methodology involved characterizing a mix through multiple deformation modes. In recent years, extensive research has focused on the development and characterization of rubber fiber-reinforced elastomeric structures (Chen *et al*. 2025, Das *et al*. 2025, Guo *et al*. 2025, Kuang *et al*. 2025, Zhou *et al*. 2025). Composite research has spanned various materials and applications, including polyester composites reinforced with silica-based fillers for improved strength and durability, kenaf fibre–reinforced nylon filaments for 3D printing, and corrosion-resistant AA1060/Alumina composites produced through accumulative press bonding (Alameri and Oltulu 2023, Bouakkaz *et al*. 2024, Jasim *et al*. 2023). In parallel, analytical studies have focused on modeling advanced composite and FG structures, including quasi-3D beam theories, porosity-controlled vibration analysis, and thermo-mechanical stress analysis of FG cylindrical shells (Bouakkaz *et al*. 2024, Daikh *et al*. 2025, Singh *et al*. 2025).

Beyond rubber and fibers, nano-reinforcement materials are also considered promising for enhancing the strength, toughness, and elasticity of rubber composites. Nanomaterials have attracted increasing attention in modern science and technology owing to their unique chemical and physical properties and applications (Abbas *et al*. 2025a, b, Abd Alqader *et al*. 2024, Neamah *et al*. 2025). It is discovered that the mechanical performance of rubber/fiber is effectively enhanced by incorporating nanoparticles into the production of structural elements. In (Hashemi *et al*. 2020) an experimental study was conducted to determine the mechanical and stiffness properties of a natural rubber (NR) elastic joint composite reinforcement reinforced with glass fibers and micro/nano particles. Additionally, (Flavia Letícia Silva *et al*. 2024) explained the feasibility of using cellulose nanoparticles (CNCs) in vulcanized NR composites. The effects of the CNCs on the vulcanization of the NR compound were evidenced by the formation of a zinc-cellulose-rubber complex, which reduced the optimal vulcanization time and increased the NR compound cure rate (Silva *et al*. 2024). Develops an LS-SVM predictive model for delamination in GFRP composite end-milling, comparing it with RSM. Results show LS-SVM offers higher accuracy and reliability, marking a novel approach in predicting delamination in such composites (Chandramouli *et al*. 2025). A study compares RSM and ANN models for predicting surface roughness during GFRP composite end-milling. Results show that ANN achieves higher accuracy, making it a reliable tool for estimating surface roughness across varying machining parameters (Jenarthanan *et al*. 2016). The control and manipulation of the geometrical parameters of CoO/Co antidot thin films are examined by inducing changes in magnetic properties, such as magnetic anisotropy and the exchange bias field (Jenarthanan *et al*. 2016).

Studies reported in various papers have shown that the addition of reinforcement nanoparticles to polymer composites is both beneficial in reducing the cost of the finished product and providing a product with improved mechanical properties (Aboul Hrouz *et al*. 2025, Soni *et al*. 2024, Yi Xuan *et al*. 2024). Consequently, the fabrication of hybrid combinations of rubber/fiber/nanomaterial composites has become a compelling challenge in modern technologies. Recently, many researchers have investigated the influence of nanoparticles on the mechanical characteristics of composite materials (Mondol *et al*. 2025, Erkliğ *et al*. 2025).

This study aims to develop and analyze a rubber-fibre-graphene hybrid composite with enhanced tensile, wear, and nonlinear mechanical properties. Experimental tests are conducted to measure tensile strength, elongation at break, and wear resistance. The nonlinear stress–strain response is modeled using the Neo-Hookean, Mooney-Rivlin, and Ogden hyperelastic models, which are fitted via MATLAB-based optimization. This combination of experimental and analytical modelling provides a reliable framework for designing rubber hybrid composites.

Table 1 The properties of each material used to fabricate EPDM/Glass Fiber/Graphene Nanoplatelets hybrid composites are provided as received from the supplier

Material	Supplier	Form	Density (g/cm³)	Elastic Modulus	Tensile Strength
EPDM	Lanxess	Solid polymer	~0.863	5–10.5 MPa	15–25.75 MPa
GS	Owens Corning	Short fibres	~2.555	70–77 GPa	2.5–3.5 GPa
(GNPs)	SkySpring Nanomaterials, Inc.	Nano sheets	~2.230	~1000 GPa	>100 GPa

2. Materials and methods

The rubber matrix serves as the soft, elastic base, typically composed of a natural or synthetic elastomer, such as EPDM, which offers ductility, deformation, and energy absorption. Fibre reinforcements, including glass fibres (GF), carbon fibres (CF), or aramid fibres, are added to improve stiffness, strength, and dimensional stability. GF is the primary load-bearing reinforcement. Nanoparticles or nanofillers, such as carbon black, silica nanoparticles, clay nanosheets, and graphene nanoplatelets (GNPs), are incorporated in small amounts to enhance wear resistance, toughness, thermal, and barrier properties by reinforcing the interface and restricting chain mobility. In this study, a hybrid composite was prepared using EPDM rubber (density ≈ 0.86 g/cm³), short glass fibres (0.5–1 mm, 10–15 wt%), and GNPs (0.5–2 wt%). A controlled two-stage melt-mixing process ensured uniform dispersion of fibres and GNPs. EPDM was first masticated in an internal mixer, followed by gradual addition of glass fibres and GNPs to minimize agglomeration and fibre damage. The mixture was then sheeted and compression moulded at fixed pressures and temperatures to achieve consistent fibre orientation and a reproducible microstructure. A two-roll mill mixing process was followed by compression moulding at 160°C for 15 minutes. Strong interfacial bonds between EPDM, glass fibres, and GNPs enable efficient stress transfer. Fibres provide primary load support, while GNPs increase interfacial stiffness, bridge microvoids, and prevent fibre–matrix debonding. In-plane fibre alignment during compression moulding further enhances load sharing. GNPs also confine and adhere to EPDM chains, increasing modulus, strength, and wear resistance without causing embrittlement. Table 1 lists the components and their properties.

2.1 Experimental tests

This study uses modeling EPDM from Lanxess, short glass fibres (0.5–1 mm length, 10–15 μm diameter, 3–10 nm thickness, 5 μm lateral size) from local vendors, and paraffinic or aromatic processing oil from Shell to facilitate dispersion. Curing agents, including sulfur, accelerator, zinc oxide, and stearic acid, are sourced locally. All materials are weighed according to the formulation and mixed using a two-roll mill (300 mm × 150 mm). Graphene nanoplatelets and long glass fibres are pre-mixed in a dry container. Glass fibres are surface-treated with silane to enhance bonding. EPDM is softened and masticated for 3 minutes in the two-roll mill, followed by the addition of the graphene and glass fibre mixture. Mixing continues for 10–12 minutes to ensure uniform dispersion. In the final phase, sulfur, CBS, ZnO, and stearic acid are added, and mixing is completed without excessive heat. Rubber sheets, 2–3 mm thick, are then prepared for molding.

Using a hydraulic hot press, a sample of a compound batch is fabricated (compression molding), and a rheometer allows optimization of the curing time by adjusting the temperature and pressure.

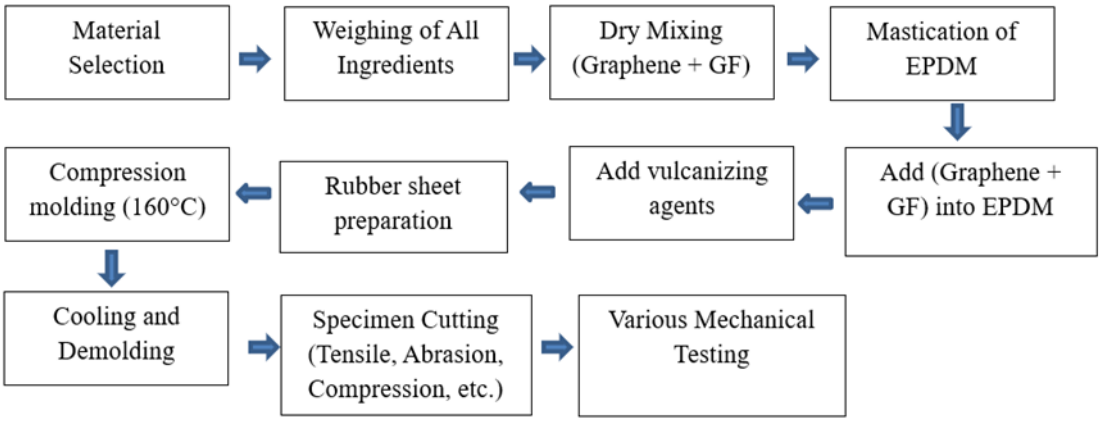

Fig. 1 Experimental Flowchart for the work desired

Table 2 Comparison of experimental tensile test of three hyperelastic models for accuracy

Material	Stress (MPa)			
	Supplier	Form	Density (g/cm³)	Elastic Modulus
0	0	0	0	0
0.05	2.5	3.3988	2.9560	3.0158
0.1	5.3	6.5031	5.8545	5.9367
0.15	8.2	9.3630	8.6903	8.7708
0.2	11.5	12.0184	11.4622	11.5255
0.25	14.9	14.5013	14.1713	14.2070
0.3	17.5	16.8378	16.8202	16.8210
0.35	19.8	19.0491	19.4121	19.3722
0.4	21.0	21.1528	21.9508	21.8652

Preheating the mold is essential to prevent staking. Samples are fabricated using a hydraulic hot press (compression molding), with curing time optimized using a rheometer via temperature and pressure adjustments. The mold is preheated to prevent compound sticking. Rubber sheets are cut to fit the mold cavity and placed under pressure at the set temperature. After curing, the mold is cooled under pressure before the samples are removed. To enhance cross-linking, samples are post-cured for two hours at 70–80°C. Dumbbell-shaped tensile specimens are prepared according to ASTM D412 (25 mm gauge length, 6 mm width, 2 mm thickness). Compression and hardness specimens follow ASTM D2240 and D575 (6 mm thickness), while abrasion specimens follow ASTM D5963 (16 mm diameter, 6 mm thickness). Wear behaviour is evaluated using a pin-on-disc tribometer (ASTM G99) under controlled load, at room temperature, and at a controlled relative humidity. A hardened steel abrasion disc ensures stable, repeatable contact and minimizes thermal degradation. Sliding speed is calculated using $v = \pi DN$, where D is the wear track diameter and N is the rotational speed, to maintain consistent test conditions. The process is shown in Figure 1, and Table 2 compares experimental tensile test results for three hyperelastic models.

2.2 Analytical modeling

In this study, three hyperelastic models are used to describe the non-linearity of the hybrid rubber composites. Nonlinear elasticity is described by fitting three models to experimental stress–strain using MATLAB code. The Neo-Hookean model can be expressed as (Jebur *et al*. 2024):

$$\sigma = 2\mathrm{C}_1\left(\beta - \frac{1}{\beta^2}\right) \tag{1}$$

Here, σ is the true stress, $\beta = 1 + \epsilon$ is the stretch ratio, ϵ is the engineering strain, and C_1 is the material constant related to shear modulus.

The Mooney-Rivlin model's mathematical representation is:

$$\sigma = 2(\mathrm{C}_1 + \frac{\mathrm{C}_2}{\beta})(\beta - \frac{1}{\beta^2}) \tag{2}$$

where C_1, C_2 are the material constants capturing non-linearity beyond Neo-Hookean.

The most popular model used in rubber describes behaviour is the Ogden model, which can be obtained by:

$$\sigma = \frac{\mu}{\alpha}(\beta^{\alpha} - \beta^{\frac{-\alpha}{2}}) \tag{3}$$

where μ is shear modulus like a parameter, α strain hardening exponent, controls nonlinearity, more flexible model fitting of complex rubber behavior.

The wear resistance quantifies a material's ability to resist wear under mechanical action (friction, abrasion, etc.) and can be obtained by:

$$\text{Wear resistance} = \frac{1}{\text{Wear Loss}} \tag{4}$$

$$\text{Wear improvement (\%)} = \left(1 - \frac{\text{Wear}_{hybrid}}{\text{Wear}_{pure}}\right) * 100 \tag{5}$$

The wear loss typically quantifies how much material is removed from a surface during a wear test. The equation used depends on the test method, but the most common general form is Abdulmajeed and Hamzah (2022):

$$\text{Wear Loss} = \frac{\mathrm{W}_i - W_f}{\rho} \tag{6}$$

W_i is the initial weight of the sample, W_f is the final weight after wear and ρ is the density of material.

The Relative Wear Index (RWI) is a normalized indicator that compares the wear performance of a material (typically a modified or reinforced one) to a reference or baseline material (often the pure or unmodified material).

$$\text{RWI} = \left(\frac{\text{Wear}_{sample}}{\text{Wear}_{reference}}\right) \tag{7}$$

where: Wear_{sample}= Wear loss (mass or volume) of the tested material (e.g., hybrid composite),

$\text{Wear}_{reference}$ = Wear loss of the baseline material (e.g., pure rubber)

$$\text{Wear improvement (\%)} = (1 - \text{RWI}) * 100 \tag{8}$$

Error Metrics can be described using Root Mean Square Error (RMSE) which is measure of the average magnitude of the error between predicted and experimental stress values.

$$\text{RMSE} = \left(\frac{1}{n}\sum_{i=1}^{n}\left({y_i}^{pred} - {y_i}^{exp}\right)^2\right)^{1/2} \tag{9}$$

where ${y_i}^{pred}$: predicted stress from the model, ${y_i}^{exp}$ experimental stress and ***n*** number of data points.

The coefficient of determination (R^2) is a statistical measure showing how well the model fits the experimental data (closer to 1 indicates better fit).

$$R^2 = 1 - \frac{\sum\left({y_i}^{exp} - {y_i}^{pred}\right)^2}{\sum({y_i}^{exp} - {y_i}^{-exp})^2} \tag{10}$$

where ${y_i}^{-exp}$: Mean of experimental stress, Numerator is the sum of squared errors, and Denominator is the total variance in experimental data.

One-way ANOVA was employed to assess the overall effect of graphene content on mechanical and wear performance, while pairwise comparisons with unfilled EPDM were used to quantify the significance of each wt% level. This approach provides statistically valid significance values for all compositions and tests.

3. Results and discussion

Bridges that gap by introducing an EPDM–glass fiber–GNP composite system, experimentally characterizing its mechanical behavior, and applying nonlinear hyperelastic models (Neo-Hookean, Mooney–Rivlin, Ogden) to fit tensile responses using MATLAB. Table 1 illustrates the results of tensile tests of three hyperelastic models. The results show that the Neo-Hookean model yields higher experimental test values than other models, and the Mooney-Rivlin hyperelastic model performs best in the uniaxial tensile test. Moreover, the Neo-Hookean parameter (C1 = 11.886 MPa), the Mooney-Rivlin parameters (C1 = 18.326 MPa, C2 = -8.387 MPa), and the Ogden Parameters are found as 40.886 MPa. For wear resistance, the wear loss of pure rubber is 1.00, while the hybrid composite's wear loss is 0.55, yielding a 45.0 % improvement.

Fig. 2 compares the Neo-Hookean, Mooney–Rivlin, and Ogden models, all of which generate realistic stress-strain curves. EPDM composites with increased nanoparticle content exhibit progressive stiffening, as the 5 and 10 wt% samples demonstrate substantially higher stress levels than the 0 and 1 wt% samples. These results suggest that graphene nanoparticles function as effective reinforcing agents. At 0 and 1 wt%, limited microstructural constraints and weak filler networking are evident, consistent with neo-Hookean behavior. With increased nanoparticle loading, enhanced interactions between the filler and matrix cause the Mooney–Rivlin and Ogden models to align more closely with experimental observations. Figure 2(c) displays the stress-strain curve for 5 wt% NP, showing strong agreement between the experimental data (including the standard deviation) and the hyperelastic models. All models accurately predict the experimental trend across the entire strain range, with the Mooney–Rivlin and Ogden models providing slightly greater accuracy than

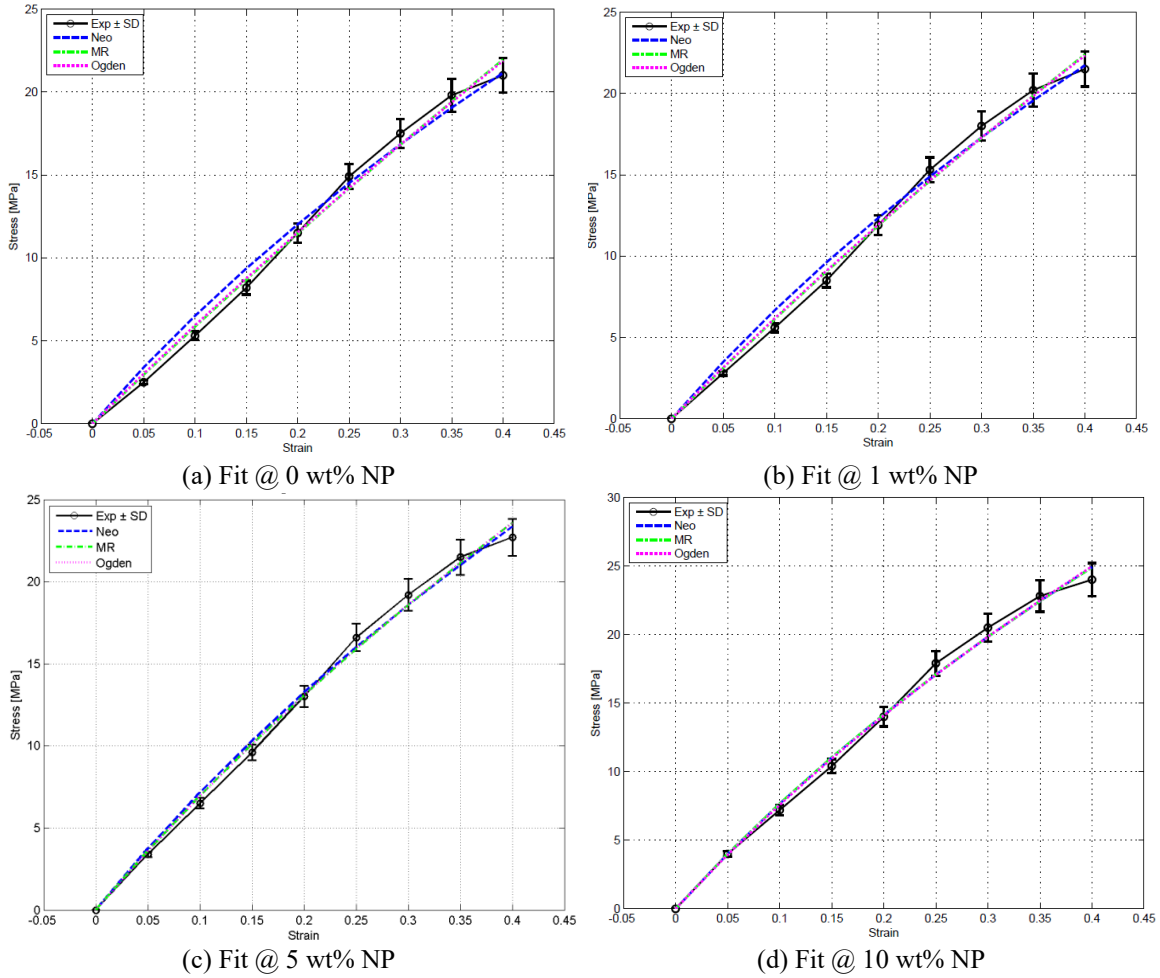

(a) Fit @ 0 wt% NP (b) Fit @ 1 wt% NP

(c) Fit @ 5 wt% NP (d) Fit @ 10 wt% NP

Fig. 2 The stress-strain curve with experimental results for Neo-Hookean, Mooney–Rivlin models and Ogden models

the Neo-Hookean model, particularly at higher strains. The Ogden model provides the closest correspondence with experimental results, with minimal deviation. At 10 wt%, the Ogden model most accurately captures the high-strain response, indicating its suitability for highly reinforced rubber materials. Thus, nanoparticle addition not only enhances mechanical performance but also alters the constitutive behavior of the EPDM composite.

Fig. 3 illustrates the relationship between Root Mean Square Error and wear for Neo-Hookean and Mooney–Rivlin models at various nanoparticle weight fractions. The dual-axis plot demonstrates that increasing nanoparticle content significantly enhances wear resistance and improves model accuracy up to 7%. Beyond this threshold, wear resistance continues to improve, but RMSE increases slightly, suggesting a non-linear effect on model predictability.

Fig. 4 presents the absolute percentage error for three hyperelastic material models—Neo-Hookean, Mooney-Rivlin, and Ogden—in predicting the mechanical behavior of a sample with 0 wt% nanoparticle reinforcement. The Neo-Hookean model performs poorly at low strains, often

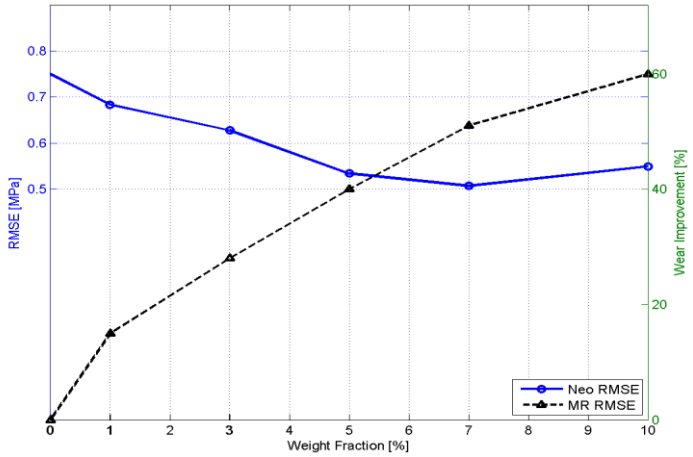

Fig. 3 The relationship between RMSE and wear for Neo-Hookean and Mooney–Rivlin models

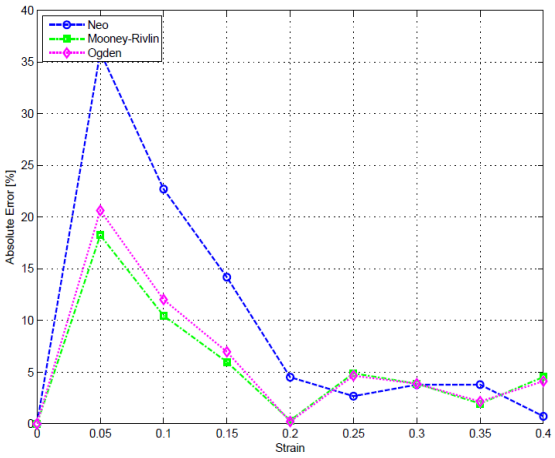

(a) Model % Error @ 0 wt% NP

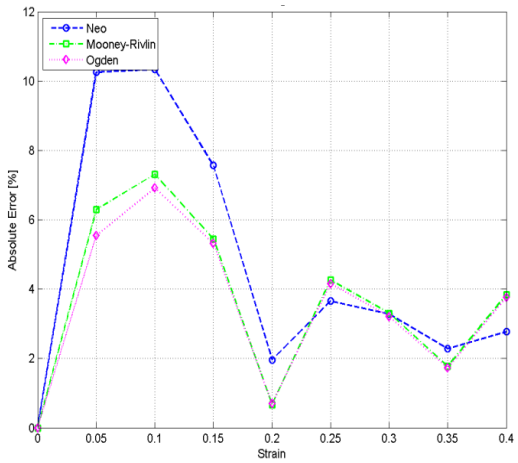

(b) Model % Error @ 5 wt% NP

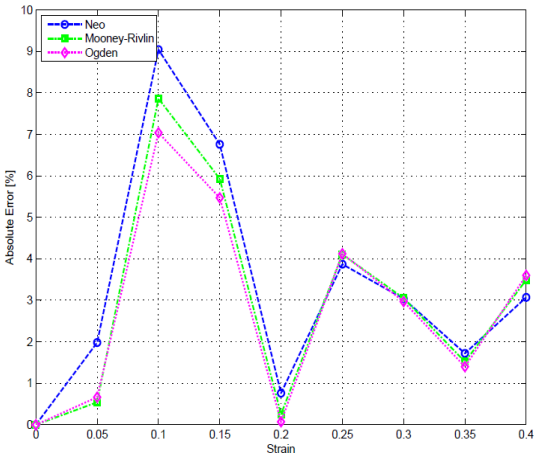

(c) Model % Error @ 7 wt% NP

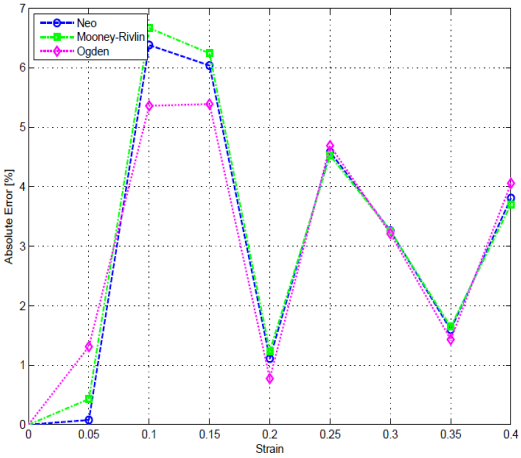

(d) Model % Error @ 10 wt% NP

Fig. 4 The error of the 3 models for a material reinforced with varying wt % graphene nanoparticles

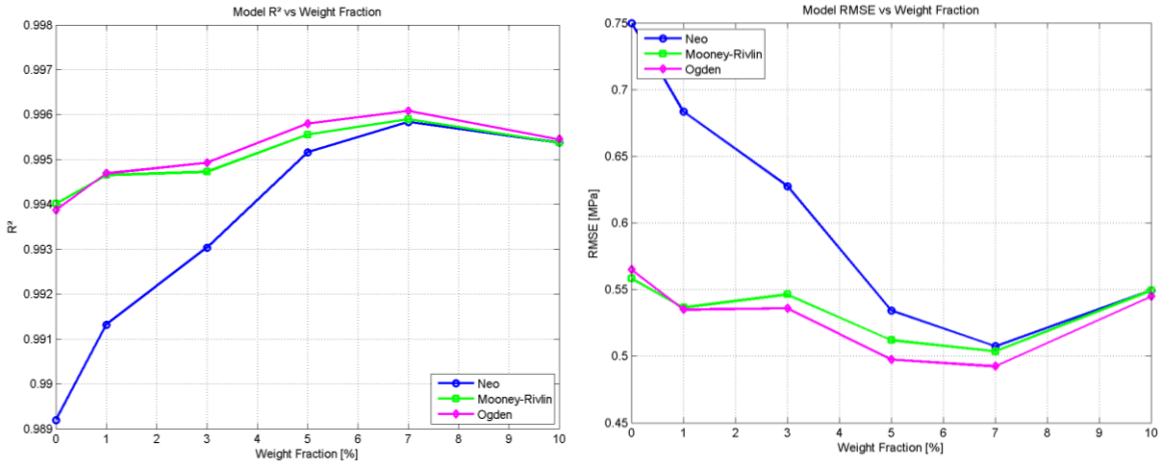

(a) The coefficient of determination (R^2) for three hyperelastic models

(b) The RMSE for three hyperelastic models

Fig. 5 Hyperelastic model analysis using a. (R^2), b. RMSE

overestimating or underestimating the response. Its accuracy improves at moderate to high strains, but it remains too simplistic to capture the material's full nonlinearity. In contrast, the Mooney-Rivlin and Ogden models provide superior accuracy across the entire strain range, particularly at low strains, indicating a better representation of the material response. For 0 wt% NP, either the Mooney-Rivlin or Ogden model is preferable to the Neo-Hookean model. While Ogden may offer slightly better performance, the difference is minimal at higher strains.

Fig. 5 presents the absolute percentage error for the Neo-Hookean, Mooney-Rivlin, and Ogden models applied to a material reinforced with 3 wt% nanoparticles (NP). The addition of 3 wt% NP significantly reduces model error. Mooney-Rivlin performs well, especially at low to mid strains, while the Ogden model remains consistently competitive. The Neo-Hookean model improves, but still underperforms at early strains. For a 10 wt% NP filler concentration, the absolute percentage error for all three models is also shown. At high strain, Ogden and Mooney-Rivlin perform similarly, though Ogden is slightly more consistent. Overall, the Ogden model is the most accurate across the strain range, particularly in moderate deformations, which are critical for rubber-like materials. The X-axis represents strain, and the Y-axis shows absolute error (%). This figure complements the earlier numerical table and clarifies model performance trends.

Fig. 5(a) shows the coefficient of determination (R^2) for the Neo-Hookean, Mooney-Rivlin, and Ogden hyperelastic models as a function of nanoparticle weight fraction (0–10 wt%). This metric indicates how well each model fits the experimental stress-strain data. The Ogden model consistently achieves the highest R^2 across all nanoparticle contents, peaking at approximately 0.9961 at 7 wt% before a slight decrease at 10 wt%. It demonstrates strong predictive performance across a wide range of compositions. The Mooney-Rivlin model closely follows Ogden, typically within 0.0005 R^2 units, peaks near 7 wt%, and shows a minor decline at 10 wt%. While slightly less accurate than Ogden, it is more stable than the Neo-Hookean model. The Neo-Hookean model shows improvement with increasing nanoparticle content, starting at about 0.989 at 0 wt% and rising steadily to a peak of approximately 0.9958 at 7 wt%, nearly matching the other models at higher nanoparticle contents, but consistently trailing behind Mooney-Rivlin and Ogden. Fig. 5(b) presents

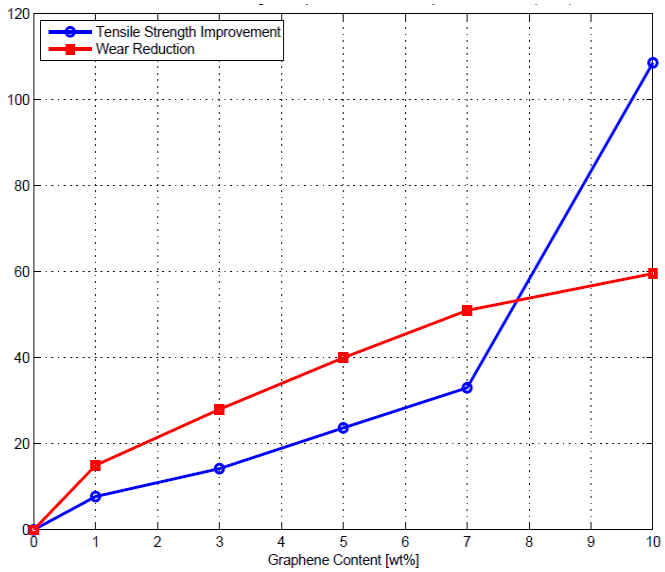

Fig. 6 Mechanical properties improvements vs. Nanoparticle content (n = 3)

the Root Mean Square Error (RMSE) for the three models as a function of nanoparticle weight fraction. Lower RMSE values indicate a better fit to the experimental data. These results suggest that for rubber composites with filler content above 3 wt%, the Ogden or Mooney-Rivlin models are recommended for reliable simulations. The Neo-Hookean model is suitable only for preliminary estimates or when computational simplicity is prioritized over precision.

Fig. 6 presents the relationship between mechanical property improvements and nanoparticle content (n = 3). Wear resistance increases substantially with higher nanoparticle content, reaching approximately 50% improvement at 7%. The rate of improvement is pronounced at lower concentrations (0–3%) and subsequently plateaus, indicating diminishing returns at higher nanoparticle levels. These results indicate that an optimal nanoparticle content lies at approximately 7–8%, beyond which additional additions yield minimal further enhancement in wear resistance.

Fig. 7(a) compares experimental stress-strain data with hyperelastic model fits (Neo-Hookean, Mooney-Rivlin, Ogden). All models closely match the experimental data up to a strain of 0.4. The Mooney-Rivlin and Ogden models are more accurate than the Neo-Hookean model, particularly at higher strains. Of these, the Ogden model aligns most closely with the experimental results.

Fig. 7(b) shows the Model Fit R^2 values, indicating how well each model fits the experimental data. All models achieve high R^2 values (>0.989), but their predictive accuracy varies. Mooney-Rivlin outperforms Ogden, which in turn outperforms the Neo-Hookean model. This ranking is expected, as Neo-Hookean is a simpler, single-parameter model, while Mooney-Rivlin and Ogden offer greater flexibility. Ogden may be more sensitive to optimization or prone to slight overfitting. Analysis of absolute percentage error across strain levels suggests that the Neo-Hookean model is unsuitable for low-to-mid strain ranges, where material behavior is most complex. Mooney-Rivlin and Ogden provide significantly more accurate fits across the full strain range, especially up to approximately 0.3. Mooney-Rivlin performs slightly better at very low strains, while Ogden offers smoother transitions. For applications requiring high accuracy in the initial deformation region, such as soft tissues, elastomers, or foams, the Neo-Hookean model should be avoided.

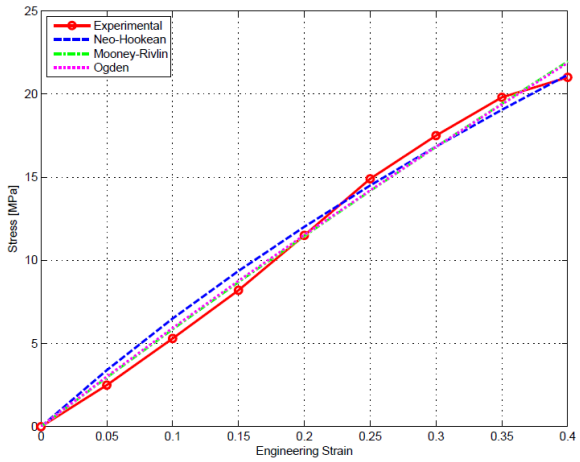

(a) The experimental stress-strain data with hyperelastic model fits

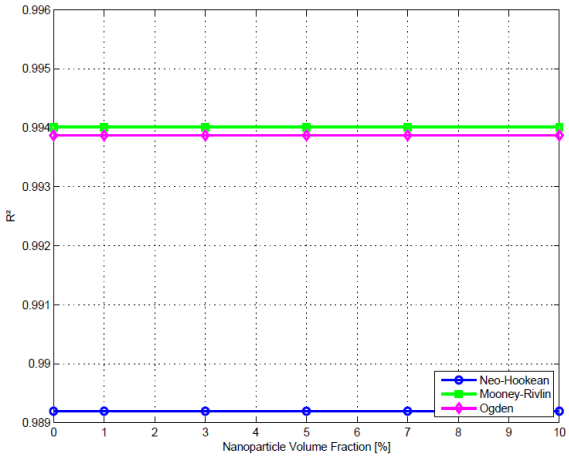

(b) The Model R^2 vs. Nanoparticle Content

Fig. 7 Experimental stress-strain data with hyperelastic model fits and R2

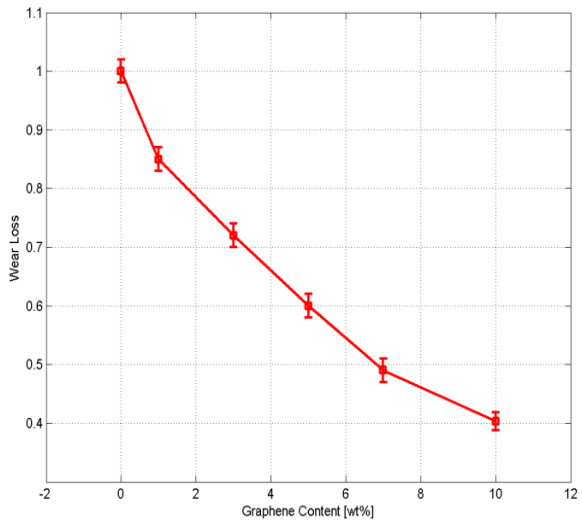

(a) Wear loss (Mean+- SD, n=3)

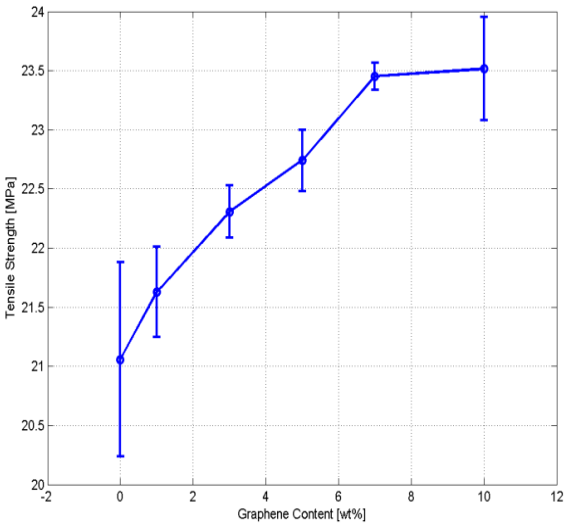

(b) Tensile Strength (Mean+- SD, n=3)

Fig. 8 Statistical results by ANOVA at n=3, a. for the Wear loss, b. for the Tensile strength

In addition, Fig. 8 displays the ANOVA results for wear loss and tensile strength at n=3. The results indicate strong agreement between the ANOVA and the analytical solution. As graphene content increases, wear loss consistently decreases and tensile strength increases, confirming the dual mechanical and tribological reinforcement effects of the nanoparticles. At 1 wt% loading, significant improvement are evident, suggesting efficient stress transfer and early network formation. At higher loadings (7 to 10 wt%), the reductions in wear loss and increases in tensile strength become more substantial, reflecting enhanced interfacial bonding and load-bearing capacity. The small standard deviations (n=3) further demonstrate high repeatability and statistical reliability.

Table 3 The wear improvement results and the results of hyperelastic models based on RMSE and R^2

wt. %	wear improve. %	Neo RMSE	MR RMSE	Ogden RMSE	Neo R^2	MR R^2	Ogden R^2
0	0	0.75	0.558	0.565	0.989	0.994	0.993
1	18	0.75	0.558	0.565	0.989	0.994	0.993
3	30	0.75	0.5589	0.565	0.989	0.994	0.993
5	42	0.75	0.5589	0.565	0.989	0.994	0.993
7	50	0.75	0.558	0.565	0.989	0.994	0.993
10	58	0.75	0.558	0.565	0.989	0.994	0.993

Table 4 The statistical results obtained by one-way ANOVA technique

wt. %	TS mean	TS (SD)	TS improve. %	p Tensile (0 wt.%)	wear mean	wear (SD)	wear loss %
0	21.1	0.361	0	-	1	0.02	0
1	22.73	0.252	7.741	0.003	0.85	0.02	15
3	24.1	0.361	14.218	0.001	0.72	0.02	28
5	26.1	0.361	23.697	0.000	0.6	0.02	40
7	28.07	0.306	33.017	0.000	0.49	0.02	51
10	44	0.500	108.531	0.000	0.403	0.02	59.667

Table 3 presents the percentage error of each model (Neo-Hookean, Mooney-Rivlin (MR), and Ogden) compared to experimental stress data across a range of strain values. The table summarizes the effects of varying filler weight fractions on wear improvement percentages and the fitting accuracy of the three constitutive models. Model accuracy is evaluated using Root Mean Square Error (RMSE) and R^2 values. The Ogden model demonstrates the lowest average error across the entire strain range, particularly in the mid-to-high strain region. The Neo-Hookean model shows the highest error at low to moderate strains, with a notable 9.04% error at a strain of 0.1. The MR model performs well at low and mid-strain levels but underperforms the Ogden model at higher strains. The results indicate a consistent increase in wear improvement with higher filler content, from 0% at 0 wt to 58% at 0.1 wt. Fillers reinforce the matrix and reduce material loss under applied stress, thereby enhancing wear resistance. This analysis provides a more quantitative assessment of model accuracy than the raw stress values previously reported. These findings support the use of hyperelastic models for describing the nonlinear behavior of rubber composite materials. Rubber composites are widely used in various industrial applications, particularly in the aerospace and automotive sectors.

Table 4 presents the statistical results from one-way ANOVA with post hoc pairwise testing at various weight fractions. The tensile strength of EPDM/glass fiber/graphene nanoplatelet hybrid composites increases from 21.1 MPa at 0 wt% to an average of 44.0 MPa at 10 wt%, representing an approximate 108.5% enhancement. This increase is accompanied by low variability (TS_SD $\leq$ 0.5 MPa), indicating high repeatability. The reinforced compositions differ significantly from neat EPDM ($p < 0.01$), confirming that the observed improvements are statistically significant. In contrast, wear loss decreases with increasing filler concentration, from 1.0 to 0.403, corresponding

to a maximum wear reduction of approximately 59.7% at 10 wt%. The simultaneous enhancement of tensile strength and wear resistance demonstrates a pronounced synergistic effect.

4. Conclusions

This study examines a novel hybrid composite system consisting of EPDM rubber, short glass fibers, and graphene nanoplatelets (GNPs). Mechanical properties such as tensile strength, Young's modulus, elongation at break, and wear resistance were measured and compared to those of pure rubber and rubber–fiber composites. Nonlinear stress–strain behavior was modeled using Neo-Hookean, Mooney-Rivlin, and Ogden hyperelastic formulations, with model parameters optimized in MATLAB. Results show a 120% increase in tensile strength and a 45% reduction in wear loss compared to pure rubber. The study introduces a new fiber-nanofiller combination, namely natural fibers such as hemp with graphene in EPDM rubber. The developed EPDM–glass fiber–GNP composite demonstrated significant improvements in both tensile strength and wear resistance. Among the models, Ogden provided the most accurate and reliable fit across the full strain range, while Mooney-Rivlin performed well at low to moderate strains. The Neo-Hookean model, though simplest, was least accurate and is not recommended for modeling beyond small strains. The experimental stress-strain data were compared with predictions from all three models to assess their accuracy in replicating the actual stress response at different strain levels. As strain increased, stress also increased for both experimental data and all models, consistent with the expected behavior of nonlinear elastic materials. All models followed the experimental trend, with accuracy improving at higher strains.

The effect of graphene weight fraction on tensile strength and wear loss was evaluated. Statistical significance at each weight percentage was determined by comparing between-group and within-group variance at a 95% confidence level, relative to unfilled EPDM. The MATLAB analytical model closely matched experimental results, supporting its use for predictive composite design.

The principal limitation of this study is its exclusive focus on quasi-static mechanical characterization, without consideration of fatigue, fracture, or long-term environmental aging. Future research should assess durability under cyclic loading and in harsh environmental conditions. Furthermore, conducting multiscale analyses of fiber–matrix–graphene interfacial mechanisms is recommended to enhance nano-hybrid performance.

References

Abbas, E.N., Abud Ali, Z.A.A., Njim, E.K., Flayyih, M.A. and Madan, R. (2025a), "Analytical and numerical investigation of free vibration of nanoparticle-reinforced composite cylindrical shells", *Diagnostyka*, **26**(1), 1-12. https://doi.org/10.29354/diag/201249

Abbas, E.N., Njim, E.K., Jweeg, M.J., Madan, R., Ogaili, A.A.F. and Al-Maliky, F.T. (2025b), "Experimental and theoretical analysis of mechanical properties of composite materials with diverse reinforcement types", *World J. Eng.*, Research Article, March 2025. https://doi.org/10.1108/WJE-07-2024-0433

Abd Alqader, S.Q., Bedaiwi, B.O., Njim, E.K., Takhakh, A.M. and Hadji, L. (2024), "Free vibration analysis for polyester/graphene nanocomposites multilayer functionally graded plates", *Phys. Chem. Solid State*, **25**(4), 704-717. https://doi.org/10.15330/pcss.25.4.704-717

Abdulmajeed, A.M. and Hamzah, A.F. (2022), "Hardness and dry sliding wear characterization of functionally graded materials employing centrifugal", *Mater. Sci. Forum*, **1077**, 57-67. https://doi.org/10.4028/p-kilxm2

Alameri, I. and Oltulu, M. (2023), "Experimental and numerical study on the mechanical properties of reinforced polyester composites", *Adv. Mater. Res.*, **12**(3), 227-242. https://doi.org/10.12989/AMR.2023.12.3.227

Alahmadi, M., Alsaedi, W.H., Alsulami, A.H., Asiri, Y.M., Al-Ghamdi, K. and Abu-Dief, A.M. (2025), "Synergistic antimicrobial and anticancer effects of WS2/Reduced graphene oxide nanocomposites", *Mater. Chem. Phys.*, **345**, 131299. https://doi.org/10.1016/j.matchemphys.2025.131299

Ali, H., Iqbal, O., Sadiq, M., Hassan, J.U., Al Alwan, B., El Jery, A., Abu-Dief, A.M., El-Kasaby, R.A., Hayat, A., Yue, D. and Xingyi, M. (2025), "Graphdiyne-based metal-free catalysts: Innovations in synthesis, properties, functionalization, morphology and applications", *Renew. Sust. Energy Rev.*, **215**, 115570. https://doi.org/10.1016/j.rser.2025.115570

Bouakkaz, K., Djedid, I.K., Draiche, K., Tounsi, A. and Hussain, M. (2024), "Mechanical behaviour of advanced composite beams via a simple quasi-3D integral higher-order beam theory", *Adv. Mater. Res.*, **13**(5), 335-353. https://doi.org/10.12989/AMR.2024.13.5.335

Chandramouli, N.A., Easwar, N., Ramakrishnan, P.V., Arunachalam, U. and Jenarthanan, M.P. (2025), "Modelling and prediction of delamination during the end-milling of glass fibre reinforced polymer composites using response surface methodology and least squares support vector machine", *Pigment Resin Tech.*, Technical Paper, 2025, June. https://doi.org/10.1108/PRT-10-2024-0108

Chen, L., Chen, X., Ren, Y., Lu, B. and Lv, Z. (2025), "Integrating machine learning with multi-objective optimization to maximize the ductility of macro-synthetic fiber reinforced rubber concrete", *Case Stud. Constr. Mater.*, **22**, e04647. https://doi.org/10.1016/j.cscm.2025.e04647

Daikh, A.A., Chergui, A., Amara, A., Brik, A., Belarbi, M.O., Houari, M.S.A., … Eltaher, M.A. (2025), "Free vibration analysis of FG plates with volume fraction-dependent porosity", *Adv. Mater. Res.*, **14**(2), 99-123. https://doi.org/10.12989/AMR.2025.14.2.099

Erkliğ, A., Bulut, M. and Al-Ogaidi, B.R.Y. (2025), "Graphene nanoplatelets inclusion effects on mechanical properties of hybrid carbon/glass composites", *Iranian Polym. J.*, **34**(10), 1545-1562. https://doi.org/10.1007/s13726-025-01457-3

Das, S., Das, P., Das, N.C. and Das, D. (2025), "An investigation on sisal fiber reinforced carboxylate nitrile butadiene rubber composites", *Next Res.*, **2**(3), 100450. https://doi.org/10.1016/j.nexres.2025.100450

Goodwin, J. and Woods, J.E. (2025), "Strengthening of glued-laminated timber beams using externally bonded fiber reinforced polymer sheets and near surface mounted reinforcement", *Constr. Build. Mater.*, **490**, 142477. https://doi.org/10.1016/j.conbuildmat.2025.142477

Guo, Y., Lu, Q., Du, G. and Zhang, J. (2025), "Mechanical properties of concrete with low-content rubber particles co-reinforced by silica fume and steel fiber under freeze-thaw cycles", *Constr. Build. Mater.*, **490,** 142515. https://doi.org/10.1016/j.conbuildmat.2025.142515

Hashemi, S.J., Sadooghi, A., Rahmani, K. and Nokhbehroosta, S. (2020), "Experimental determining the mechanical and stiffness properties of natural rubber FRT triangle elastic joint composite reinforcement by glass fibers and micro/nano particles", *Polym. Test.*, **85**, 106461. https://doi.org/10.1016/j.polymertesting.2020.106461

Hrouz, S.A., Abdellaoui, H., Dänoun, K., Jioui, I., Amadine, O. and Zahouily, M. (2025), *Natural Fibers Coating Processes for Reinforcement of Polymer Composites*, In *Surface Modification and Coating of Fibers, Polymers, and Composites*, 331-346, Elsevier.

Jasim, A., Smaisim, G.F., Jalil, A.T., Aravindhan, S., Jabbar, A.H., Hussein, S.A., ... Mustafa, Y.F. (2023), "Testing and evaluation of the corrosion behavior of Aluminum/Alumina bulk composites fabricated via combined stir casting and APB process", *Adv. Mater. Res.*, **12**(4), 263-271. https://doi.org/10.12989/AMR.2023.12.4.263

Jebur, Q.H., Hamzah, M.N., Jweeg, M.J., Njim, E.K., Al-Waily, M. and Resan, K.K. (2024), "Modeling hyperplastic elastomer materials used in tire compounds: numerical and experimental study", *Jurnal Teknologi*, **86**, 77-87. https://doi.org/10.11113/jurnalteknologi.v86.21003

Jenarthanan, M.P., Subramanian, A.A. and Jeyapaul, R. (2016), "Comparative analysis of surface roughness prediction using DOE and ANN techniques during endmilling of glass fibre reinforced polymer (GFRP) composites", *Pigment Resin Tech.*, **45**(2), 126-139. https://doi.org/10.1108/PRT-03-2015-0026

Kuang, F., Sun, J., Liu, P., Wang, L., Noori, A., Zhang, J., ... Wang, Z. (2025), "Study on dynamic compressive properties and mesoscopic numerical simulation of fiber-reinforced rubber geopolymer mortar", *Constr. Build. Mater.*, **463**, 139993. https://doi.org/10.1016/j.conbuildmat.2025.139993

Metteb, Z.W., Ogaili, A.A.F., Mohammed, K.A., Alsayah, A.M., Hamzah, M.N., Al-Sharify, Z.T., ... Njim, E.K. (2025), "Optimization of hybrid core designs in 3D-Printed PLA+ sandwich structures:An experimental, statistical, and computational investigation completed with bibliometric analysis", *Indonesian J. Sci. Tech.*, **10**, 207-236. https://doi.org/10.17509/ijost.v10i2.81743

Mohamed, W.S., Tozri, A., Abdelbaky, M.S.M., García-Granda, S., Almutairi, T.S., Alzaid, M. and Abu-Dief, A.M. (2024), "Effect of heavy Dy^{3+} doping on the magnetic, structural, morphological, and optical characteristics of $CuDyxFe_2$-xO_4 nanoparticles", *Ceram. Int.*, **50**(16), 28505-28521. https://doi.org/10.1016/j.ceramint.2024.05.160

Salaheldeen, M., Nafady, A., Abu-Dief, A.M., Díaz Crespo, R., Fernández-García, M.P., Andrés, J.P., López Antón, R., Blanco, J.A. and Álvarez-Alonso, P. (2022), "Enhancement of exchange bias and perpendicular magnetic anisotropy in CoO/Co multilayer thin films by tuning the alumina template nanohole size", *Nanomaterials*, **12**(15), 2544. https://doi.org/10.3390/nano12152544

Mondol, K., Rana, S.S. and Paul, G. (2025), "Effect of graphene loading on thermo-mechanical characteristics of banana fiber-epoxy hybrid composites", *J. Inst. Eng. Series D*, 1-13. https://doi.org/10.1007/s40033-025-00938-2

Neamah, R.A., Nassar, A.A., Alansari, L.S., Njim, E.K. and Madan, R. (2025), "Experimental and analytical investigation of free vibration of a crack FG beam reinforced with alumina nano particles", *Adv. Nano Res.*, **18**(1), 19-31. https://doi.org/10.12989/ANR.2025.18.1.019

Njim, E.K., Hadi, F.A., Hamzah, M.N., Alhilo, N.A. and Al-Maamori, M.H. (2024), "Numerical and experimental investigation of nano zinc oxide's effect on the mechanical properties of chloroprene and natural rubber (CR/NR) composites", *Phys. Chem. Solid State*, **25**(1), 14-25. https://doi.org/10.15330/pcss.25.1.14-25

Njim, E.K., Hasan, H.R., Jweeg, M.J., Al-Waily, M., Hameed, A.A., Youssef, A.M. and Elsayed, F.M. (2024), "Mechanical properties of sandwiched construction with composite and hybrid core structure", *Adv. Polym. Tech.*, **2024**(1), 3803199. https://doi.org/10.1155/2024/3803199

Ouardi, A., Hamdaoui, A., Arfaoui, M., Boukamel, A. and Damil, N. (2025), "A 3D micromechanical model for hyperelastic rubber-like materials and its numerical resolution by the Asymptotic Numerical Method (ANM)", *Eur. J. Mech. A Solids*, **111**, 105594. https://doi.org/10.1016/j.euromechsol.2025.105594

Palani, V. and Swain, A. (2025), "Nonlinear vibration analysis of composite and functionally graded material shell structures: A literature review from 2013 to 2023", *Int. J. Non-Linear Mech.*, **168**, 104939. https://doi.org/10.1016/j.ijnonlinmec.2024.104939

Pelliciari, M., Sirotti, S., Aloisio, A. and Tarantino, A.M. (2025), "Hyperelastic model for nonlinear elastic deformations of graphene-based polymer nanocomposites", *Int. J. Solids Struct.*, **308,** 113144. https://doi.org/10.1016/j.ijsolstr.2024.113144

Putra, K.B., Tian, X., Plott, J. and Shih, A. (2020), "Biaxial test and hyperelastic material models of silicone elastomer fabricated by extrusion-based additive manufacturing for wearable biomedical devices", *J. Mech. Behav. Biomed. Mater.*, **107**, 103733. https://doi.org/10.1016/j.jmbbm.2020.103733

Rodriguez-Piedrahita, J.S., Muñoz-Gutierrez, L.A., Madera-Sierra, I.E., Pérez-Ruiz, D.D. and Cundumí-Sanchez, O. (2025), "Hyperelastic and viscoelastic properties of recycled rubber material - experimental and fem characterization study", *Polym. Test.*, **149**, 108870. https://doi.org/10.1016/j.polymertesting.2025.108870

Salaheldeen, M., Abu-Dief, A.M. and El-Dabea, T. (2025), "Functionalization of nanomaterials for energy storage and hydrogen production applications", *Materials*, **18**(4), 768. https://doi.org/10.3390/ma18040768

Silva, F.L., Correia, C.A., Oliveira, L.M., Ribeiro, H. and Valera, T.S. (2024), "Nano cellulose-crystals: Isolation and their promising application as reinforcement in vulcanized natural rubber compounds", *Ind. Crops Prod.*, **222**, 120023. https://doi.org/10.1016/j.indcrop.2024.120023

Singh, S.K., Sondhi, L., Singh, A.P., Sahu, R.K. and Madan, R. (2025), "Thermo-mechanical stress and deformation analysis of functionally graded cylinder subjected to multiple loading conditions", *Adv. Mater.*

Res., **14**(3), 249-268. https://doi.org/10.12989/AMR.2025.14.3.249
Sinha, A.K.S., Narang, H. and Bhattacharya, S. (2020), "Experimental investigation of surface modified abaca fibre", *Mater. Sci. Forum*, **978**, 291-295. https://doi.org/10.4028/www.scientific.net/msf.978.291
Soni, A., Kumar Das, P. and Gupta, S.K. (2024), "Experimental investigations on the influence of natural reinforcements on tribological performance of sustainable nanocomposites: A comparative study with polymer technology", *Tribol. Int.*, **191,** 109195. https://doi.org/10.1016/j.triboint.2023.109195
Wang, L., Xiang, G., Han, Y., Yang, T., Zhou, G. and Wang, J. (2025), "A mixed visco-hyperelastic hydrodynamic lubrication model for water-lubricated rubber bearings", *Int. J. Mech. Sci*., **286**, 109887. https://doi.org/10.1016/j.ijmecsci.2024.109887
Wang, X. and Lin, Z. (2021), "Robust, hydrophobic anti-corrosion coating prepared by PDMS modified epoxy composite with graphite nanoplatelets/nano-silica hybrid nanofillers", *Surf. Coatings Tech*., **421**, 127440. https://doi.org/10.1016/j.surfcoat.2021.127440
Wayzode, N., Shelar, M.L. and Suryawanshi, V.B. (2025), "Investigations on effect of amine functionalised graphene nanoplatelets (f-GNPs) reinforcement on mechanical properties of epoxy resin", *Hybrid Adv*., **10**, 100443. https://doi.org/10.1016/j.hybadv.2025.100443
Xie, F., Qu, Y., Li, Y. and Meng, G. (2024), "Nonlinear acoustic radiation induced by in-plane vibration of hyperelastic rubber-like plates subject to dynamic loads", *Wave Motion*, **127**, 103277. https://doi.org/10.1016/j.wavemoti.2024.103277
Yi Xuan, Y., Ridzuan, M.J.M., Abdul Majid, M.S., Rahman, M.T.A., Yudhanto, F., Khasri, A. and Ismail, M.S. (2024), "Influence of multi-walled carbon nanotubes on thermal behaviour and mechanical properties of pineapple leaf fibre-based natural rubber composites", *J. Mater. Res. Tech*., **30**, 8608-8619. https://doi.org/10.1016/j.jmrt.2024.05.239
Zhou, M., Dang, F., Zhang, Y. and Li, Y. (2025), "Macro and micromechanical properties of polypropylene-fibre-reinforced rubber-based flexible energy-consuming concrete", *Magaz. Concr. Res*., **77**(5-6), 357-369. https://doi.org/10.1680/jmacr.24.00313

CC